Leszek Jarecki,
***Zbigniew Lewandowski**

Mathematical Modelling of the Pneumatic Melt Spinning of Isotactic Polypropylene. Part III. Computations of the Process Dynamics

Institute of Fundamental Technological Research, Polish Academy of Sciences
Świętokrzyska 21, 00-049 Warsaw, Poland
E-mail: ljarecki@ippt.gov.pl

*) **University of Bielsko-Biala,**
Willowa 2, 43-309 Bielsko-Biala, Poland
E-mail: z.lewandowski@wp.pl

Abstract
Computer simulation of the pneumatic melt spinning of isotactic polypropylene based on the mathematical model of the process is presented. Two dynamic zones of the air jet-filament interactions along the melt blowing axis are predicted – a zone with a drawing activity of the air jets with aligned filaments in this zone, and a passive zone with the bending and coiling of the filaments. The diameter of the fibres and structure of the nonwoven should depend on the die-to-collector distance, and the zone in which the collector is located. Ranges of the zones are discussed as dependent on the initial velocity of the air jets, the melt extrusion temperature, and the molecular weight of the polymer. Axial profiles of the polymer velocity, diameter and temperature of the filament, the tensile force, tensile stress, and rheological pressure along the melt blowing axis are presented for a process with the collector located within the air-drawing zone at a fixed take-up distance. The dynamic profiles indicate a narrow axial range of air-drawing next to the spinneret.

Key words: *melt blowing, air-drawing, nonwovens, polypropylene, modelling.*

Introduction

The melt blowing of fibres in the pneumatic nonwoven formation is a two-phase process where coaxial air jets transform individual streams of a polymer melt into filaments and deposits them onto a conveyor. The process is driven by the dynamic interactions between the polymer melt extruded from the orifices in a spinning beam and the convergent air jets blown on both sides of the filaments from the slot dies. Fast uniaxial elongation of the polymer melt is a consequence of the momentum transfer between the air jets and the individual polymer streams via the friction forces. Under such conditions, the polymer streams attenuate rapidly within a short range of the processing axis by air-drawing and nonwovens of thin fibres are obtained [1 - 5]. The polymer in the melt blowing is extruded from a row of orifices evenly distributed in the spinning beam. The single row of filaments does not affects the air jets substantially, and the influence of the filaments on the jet dynamics can be omitted [6, 7].

The mathematical modelling and computer simulation of the melt air-drawing is expected to provide a convenient tool for the designing and optimisation of the melt blowing of nonwovens. Computer aided mathematical modelling of melt blowing using isotactic polypropylene has already been considered by the present authors in a series of publications [8, 9], where a two-step procedure is used. First, the dynamic fields of the air jets were determined in [8], with the absence of the filaments, taking into account the specified geometry of the spinning beam and air slot dies. The air jet fields were computed for several values of the initial air velocities, between 30 and 300 m/s at the outflow from the slot dies. Next, the mathematical modelling of the melt drawing by the air jets with a predetermined velocity, temperature and pressure fields was considered in [9]. The air velocity, temperature, and pressure profiles along the melt blowing axis are presented in [8, 10].

A steady-state, single-filament model of melt spinning with thin filament approximation was assumed, which is well-founded for the pneumatic process. The single-filament approximation was satis-

Table 1. *Shear viscosity of iPP melt, η, for different weight-average molecular weight M_w values and temperatures determined from Eq.(29) [9] and estimated values of the melt flow-rate, MFR.*

M_w, Da	η (190 °C), Pa·s	η (230 °C), Pa·s	η (300 °C), Pa·s	MFR, g/10 min
100,000	144	58	16	260
150,000	570	230	64	65
200,000	1516	611	169	24
250,000	3240	1305	360	12
300,000	6018	2425	671	6

factory because of the relatively low volume of space occupied by the single row of filaments in the air, where the screening effects in the dynamic and temperature fields of the air jets could be neglected. The air-drawing model accounts for the viscoelasticity of the polymer melt, surface tension, hydrostatic pressure, the thermal effects of viscous friction in the bulk at high elongation rates, oriented crystallisation, the effects of crystallinity in viscosity, and the relaxation time.

The mathematical models of air-drawing presented in literature by other authors [11, 12] assume a viscous polymer fluid. They do not account for the effects of viscoelasticity., important in the case of polyolefines, the viscous friction in the polymer bulk, the surface tension, the hydrostatic pressure, and the oriented crystallisation (if present). In Part II [9] of the publication series, we present a more complete air-drawing model, necessary for discussing the importance of individual materials and processing parameters in melt blowing dynamics, as well as its role in the optimisation of the process to obtain fibres and nonwovens of a desired structure. Dynamic profiles of the polymer temperature, velocity, elongation rate, tensile force, tensile stress, hydrostatic pressure, molecular orientation, and crystallinity along the air-drawing axis are available.

Results

We present the results of computations of the dynamics of air-drawing in the melt blowing of nonwovens from isotactic polypropylene using the model presented in Part II [9] of the publication series. The set of first order differential equations obtained from Equations (4, 13, 22, 23, 34), with the boundary conditions and material parameters specified in [9], is computed for air-drawing using the standard Runge-Kutta numerical procedure [13]. Axial profiles of the polymer temperature, velocity, tensile stress, rheological pressure and degree of crystallinity are determined for several values of the initial velocity of the air jets between 30 - 300 m/s. Such a range is used due to the significant effects of the air velocity on the filament diameter and process dynamics observed in melt blowing. The melt blowing of polypropylene involves hot air jets with an initial air temperature, T_{a0}, of around 300 °C. The process is less sensitive to the initial air temperature [2], and thus a single value of T_{a0} = 300 °C is chosen for the computations. Predetermined distributions of the air jet velocity, temperature and pressure along the processing axis are used, computed and approximated by the analytical formulae in [8, 9].

The role of the material parameters of the polymer is discussed for a range of weight-average molecular weight values, M_w, between 100,000 and 300,000 (in Da units). ***Table 1*** shows the zero-shear (Newtonian) viscosity of the polymer melt, η, computed from Eq. (29) [9] for different M_w values and temperatures 190, 230, 300 °C, as well as the melt flow-rate *MFR*. The *MFR* values are determined from the zero-shear viscosity at 230 °C assuming the relation $MFR = C/\eta(230\ °C)$ and $C = 1.5\times10^4$ Pa·s [14]. For the assumed range of M_w values, the melt flow-rate is predicted to remain in the range 6 - 260 g/10 min.

The high and low initial temperatures of the polymer melt extruded from the spinneret orifices, 190 and 300 °C, are considered. The other processing parameters, i.e. the diameter of the spinneret orifice, D_0 = 0.35 mm, and the mass output per single filament, W = 0.01 g/s, are fixed.

Dynamic zones in melt blowing

Two dynamic zones along the melt blowing axis are predicted in our computations for the pneumatic process. Within the first zone, the aerodynamic interactions between individual filaments and the air jets lead to air-drawing with an intensive extension of the polymer melt along the spinning axis. The axial velocity of the air jets exceeds the velocity of the polymer in this zone, and in consequence the filaments are extended by the aerodynamic friction forces and aligned in the axial direction. The extending and aligning activity of the air friction forces vanish at a certain distance from the spinneret, and a transition to the second zone takes place at this point of the processing axis. Below this point, within the second zone, the air jet velocity is lower than the velocity of the filaments and axial motion of each filament is hampered. The aerodynamic hampering should lead to the banding and statistical coiling of the filaments, in this zone. It is also predicted by the computations that the ranges of the dynamic zones are well affected by the molecular weight and extrusion temperature of the polymer, as well as by the initial velocity of the air jets. The presence of such zones with aligned and coiled filaments on the processing axis has been reported in experimental investigations [3].

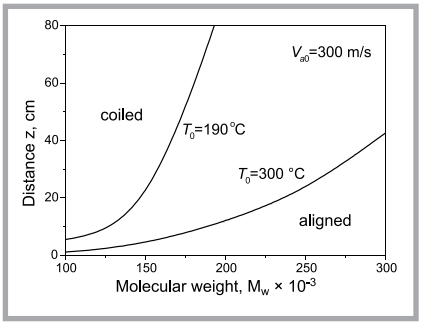

Figure 1. *Critical distance of coiling vs. M_w in the melt blowing of iPP nonwovens predicted for the initial air velocity V_{a0} = 300 m/s and melt extrusion temperatures of 190 and 300 °C. T_{a0} = 300 °C.*

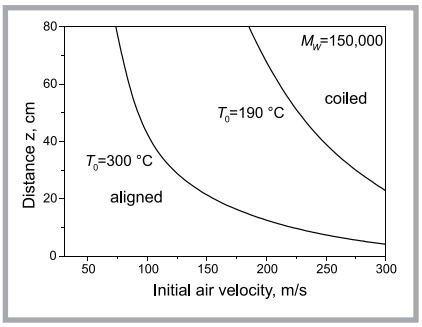

Figure 2. *Critical distance of coiling vs. initial air velocity in the melt blowing of iPP nonwovens predicted for M_w = 150,000 and melt extrusion temperatures of 190 and 300 °C. T_{a0} = 300 °C.*

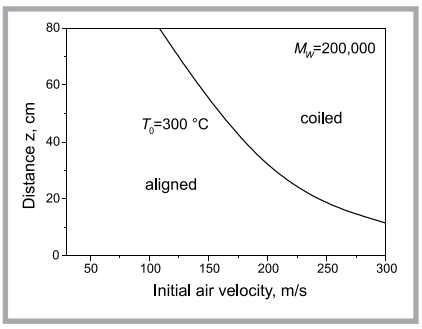

Figure 3. *Critical distance of coiling vs. initial air velocity V_{a0} in the melt blowing of iPP nonwovens predicted for M_w = 200,000 and a melt extrusion temperature of 300 °C. T_{a0} = 300 °C.*

Figures 1 - 3 illustrate the influence of the polymer molecular weight, M_w, the initial temperature of the polymer melt, T_0, and the initial velocity of the air jets, V_{a0}, on the ranges of the dynamic zones predicted in the computations. The lines in these Figures show the critical distance from the spinneret, where the

transition from the aligned to the coiled filament zone takes place. At distances smaller than the critical distance, the air jets exhibit a drawing activity leading to the aligned filaments, while at higher distances the aerodynamic hampering leads to the bending and coiling of the filaments. The critical point of bending and coiling is shifted to higher distances with an increase in the molecular weight and/or with a lowering of the melt extrusion temperature, indicating the role of the extruded melt viscosity. For example, it is predicted for polypropylene of M_w = 150,000 and initial air jet velocity V_{a0} = 300 m/s that with an increase in the melt extrusion temperature from 190 to 300 °C, the critical point of bending and coiling shifts towards the spinneret from a distance of about 23 cm to about 4 cm (***Figure 1***). The higher molecular weight of the polymer results in a higher melt viscosity and, in consequence, in a higher critical distance from the spinneret.

The influence of the initial air jet velocity on the critical distance is illustrated in ***Figures 2*** and ***3*** for the polymer molecular weight values M_w = 150,000 and 200,000, respectively, as well as for the low and high melt extrusion temperatures T_0 = 190 and 300 °C. The melt flow-rate of the polymer is 65 and 24 g/10 min, respectively (***Table 1***). With an increase in the initial velocity of the air jets, distance of bending and coiling shifts significantly towards the spinneret. In the case of a molecular weight of 150,000 and a melt extrusion temperature of 300 °C, the critical distance reduces from about 77 to 4 cm with an increase in the initial air jet velocity V_{a0} from 75 to 300 m/s (***Figure 2***). The critical distance vs. V_{a0} predicted for M_w = 200,000 and T_0 = 190 °C assumes higher values and the plot remains out of the scale of ***Figure 3***. The influence of V_{a0} on the critical distance is predicted to be stronger at higher molecular weights of the polymer. The critical distance is more sensitive to M_w and to the processing parameters at lower air jet velocities, higher molecular weights, and lower melt extrusion temperatures.

The location of the collector in one of the dynamic zones might be crucial for the nonwoven structure. If the take-up is located within the zone of aligned filaments, then the structure is controlled by the vertical velocity of the conveyor as well as by the axial velocity of the filaments deposited onto the collector. In the case of zero conveyor velocity, the orientation of the filaments in the nonwoven should be purely statistical. In the other asymptotic case, when the velocity of the conveyor equals the axial velocity of the filaments, a structure of filaments oriented along the direction of the conveyor motion should be expected. The location of the filament take-up in the coiling zone should lead to a statistically coiled and entangled structure of the nonwoven with irregularly bonded filaments, irrespective of the conveyor velocity. In this case, the structure is formed not only during the deposition of the filaments, but also during the aerodynamic coiling of the filaments on the blowing axis. Before the deposition, irregularities and the melt bonding of the filaments may appear as a consequence of interfilament contact before solidification.

In the case of the collector location, in the air-drawing zone, the diameter of the filaments in the nonwoven should depend on the take-up distance from the spinneret. The computations indicate that for obtaining nonwovens of thinner fibres within the air-drawing zone, the collector should be located closer to the critical point of bending and coiling for maximal use of the aerodynamic potential of the air jets. The take-up distances closest to the critical point and exceeding the critical point should lead to a similar thickness of the fibres, but with the effects of the spatial bending and coiling of the filaments in the case of the take-up in the coiling zone.

Axial profiles of the dynamic variables

Effective formation of fibers in the pneumatic process occurs within the air-drawing zone where extension of the polymer fluid by the air jets takes place. Beyond this zone the aerodynamic activity of the air jets is limited to slowing down the filaments, which results in their statistical banding and coiling. One can expect that the diameter of the filaments formed in the air-drawing zone is next preserved in the coiling zone, if neglecting minor thickening during possible strain relaxation. The role of material and processing parameters in the dynamics of pneumatic melt spinning affecting the final thickness of the filaments in the non-woven is discussed in this paper with respect to the take-up plane located within the air-drawing zone, at a fixed distance from the spinneret. The main parameters considered are the weight-average molecular weight, M_w, the melt extrusion temperature, T_0, and the initial velocity of the air jets, V_{a0}. The polymer mass output per single orifice, the orifice diameter, and the initial temperature of the air jets are fixed.

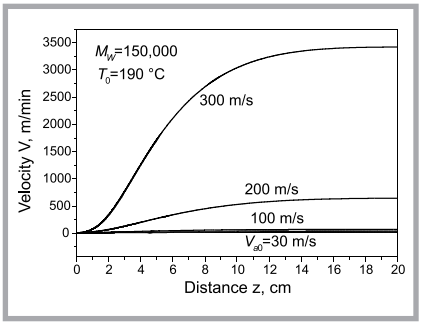

Figure 4. *Filament velocity V vs. distance z computed for different initial air velocities V_{a0} and a melt extrusion temperature of 190 °C. M_w = 150,000, T_{a0} = 300 °C.*

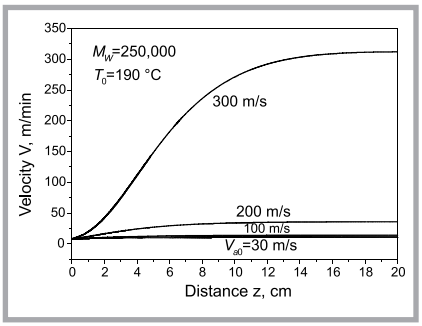

Figure 5. *Filament velocity V vs. distance z computed for different initial air velocities V_{a0} and a melt extrusion temperature of 190 °C. M_w = 250,000, T_{a0} = 300 °C.*

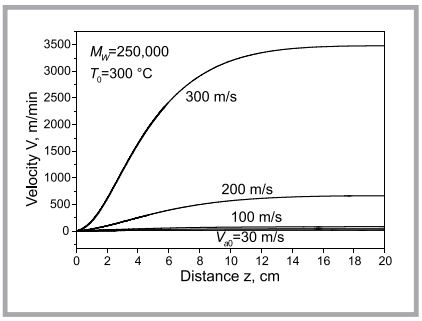

Figure 6. *Filament velocity V vs. distance z computed for different initial air velocities V_{a0} and a melt extrusion temperature of 300 °C. M_w = 250,000, T_{a0} = 300 °C.*

Axial profiles of the polymer velocity, diameter, temperature, tensile force, tensile stress, rheological pressure, and crystallinity are computed for the pneumatic melt spinning of isotactic polypropylene assuming that the take-up of the nonwoven is located at a distance of 20 cm from the spinneret. The profiles are computed for various initial velocities of the air jets, V_{a0}, between 30 and 300 m/s, two

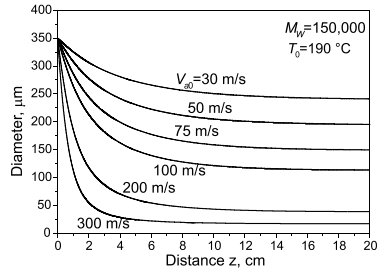

Figure 7. *Filament diameter vs. distance z computed for different initial air velocities V_{a0} and a melt extrusion temperature of 190 °C. M_w = 150,000, T_{a0} = 300 °C.*

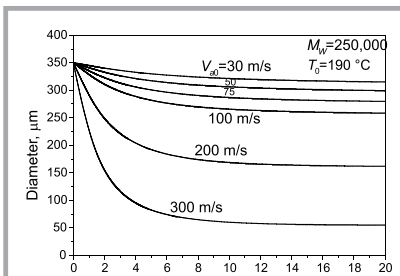

Figure 8. *Filament diameter vs. distance z computed for different initial air velocities V_{a0} and a melt extrusion temperature of 190 °C. M_w = 250,000, T_{a0} = 300 °C.*

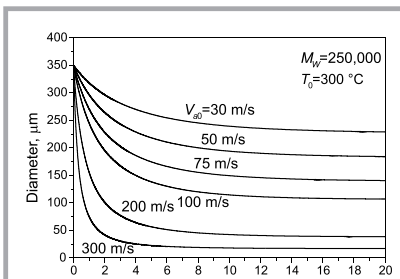

Figure 9. *Filament diameter vs. distance z computed for different initial air velocities V_{a0} and a melt extrusion temperature of 300 °C. M_w = 250,000, T_{a0} = 300 °C.*

values of the polymer molecular weight M_w = 150,000 and 250,000, as well as for the low and high melt extrusion temperatures T_0 =190 and 300 °C, providing that the take-up distance of 20 cm corresponds to the air-drawing zone in each case. The condition of the location in the air-drawing zone at this take-up distance is not satisfactory in the case of melt blowing at V_{a0} = 300 m/s from a polymer of M_w = 150,000 extruded at T_0 = 300 °C. The Newtonian shear viscosity of the polymer melt is 570 Pa·s at an extrusion temperature T_0 = 190 °C and 64 Pa·s at T_0 = 300 °C (***Table 1***). For M_w = 250,000 the values are 3240 and 360 Pa·s, respectively. These M_w values, corresponding to the *MFR* values of 12 and 65 g/10 min, are chosen to illustrate significant effects of the polymer molecular weight on the process dynamic and filament diameter.

The role of the initial air jet velocity in the axial profiles of the polymer velocity is illustrated in ***Figures 4 - 6*** and on the diameter of the filaments in ***Figures 7 - 9***. The filament velocity is presented in m/min, a unit commonly used in melt spinning research. The velocity profiles indicate that the elongation rate of the polymer (axial gradient of the velocity) show the highest values at distances of about 5 cm from the spinneret, and an effective formation of the filament (diameter) occurs within a distance range of 6 - 8 cm from the spinneret. The above ranges are not significantly affected by the initial velocity of the air jets. For a polymer of low molecular weight of M_w = 150,000 and a low melt extrusion temperature of T_0 = 190 °C, the predicted filament velocity at the take-up plane increases from 20 up to 3400 m/min with an increase on the initial air jet velocity, from 30 up to 300 m/s. The corresponding reduction in the diameter of the filaments at the take-up plane is from 240 down to 17 μm.

The significant role of the polymer molecular weight and the melt extrusion temperature in the axial profiles of the filament velocity and diameter is also illustrated. The plots shown in ***Figures 4 - 9*** indicate that a lower molecular weight and higher melt extrusion temperature lead to a higher velocity of the filaments at the take-up plane as well as thinner filaments. It is predicted, for example, that a reduction in the molecular weight from M_w = 250,000 to 150,000 leads, at a fixed melt extrusion temperature of T_0 = 190 °C and initial air jet velocity V_{a0} = 300 m/s, to a reduction in the diameter of the fibres from 55 to 16 μm. Application of a higher melt extrusion temperature T_0 = 300 °C and a polymer with a higher molecular weight of M_w = 250,000, also leads to a similar reduction in the diameter, from 55 to 17 μm at V_{a0} = 300 m/s. The effects of the molecular weight and melt extrusion temperature on the diameter exhibit such trends also for the other initial air jet velocities. Results of the computations indicate the significant role of the factors considered and are in qualitative agreement with experimental observations published in literature [1 - 5]. The influence of the initial air jet velocity, molecular weight and melt extrusion temperature on the axial profiles of the filament temperature are illustrated in ***Figures 10 - 12***. It is predicted that at the lower melt extrusion temperature T_0 = 190 °C, much below the initial air jet temperature T_{a0} = 300 °C, the polymer temperature increases along the process axis by 5 - 20 degrees, depending upon the initial air jet velocity, and achieves the maximum at a distance of about 1- 2 cm from the spinneret (***Figures 10, 11***). The increase in temperature is higher

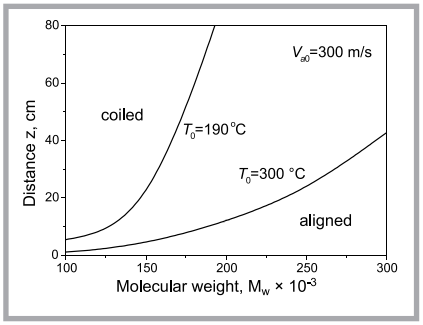

Figure 10. *Filament temperature T vs. distance z computed for different initial air velocities V_{a0} a and melt extrusion temperature of 190 °C. M_w = 150,000, T_{a0} = 300 °C.*

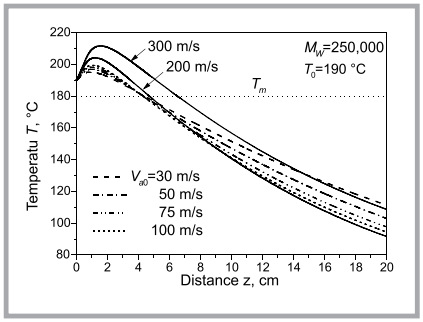

Figure 11. *Filament temperature T vs. distance z computed for different initial air velocities V_{a0} and a melt extrusion temperature of 190 °C. M_w = 250,000, T_{a0} = 300 °C.*

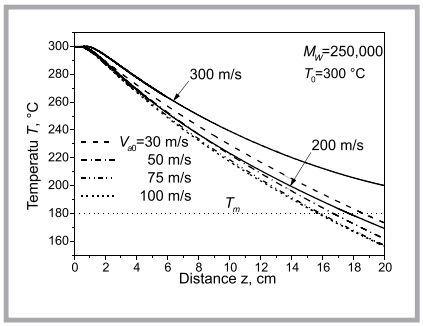

Figure 12. *Filament temperature T vs. distance z computed for different initial air velocities V_{a0} and a melt extrusion temperature of 300 °C. M_w = 250,000, T_{a0} = 300 °C.*

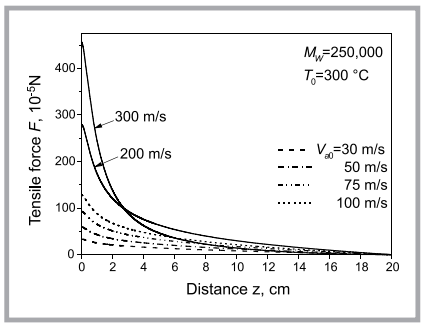

Figure 13. *Tensile force F vs. distance z computed for different initial air velocities V_{a0} and a melt extrusion temperature of 300 °C. M_w = 250,000, T_{a0} = 300 °C.*

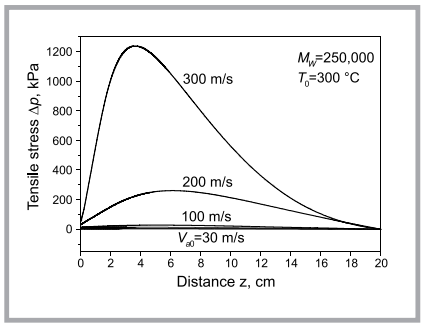

Figure 14. *Tensile stress Δp vs. distance z computed for different initial air velocities V_{a0} and a melt extrusion temperature of 300 °C. M_w = 250,000, T_{a0} = 300 °C.*

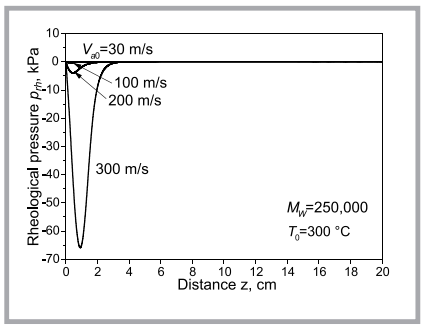

Figure 15. *Rheological pressure p_{rh} vs. distance z computed for different initial air velocities V_{a0} and a melt extrusion temperature of 300 °C. M_w = 250,000, T_{a0} = 300 °C.*

for higher initial velocities of the jets. Some effect of the molecular weight on the temperature profiles are predicted. For the process with a low melt extrusion temperature 190 °C, the maximum polymer temperature is higher by about 10% in the case of a higher molecular weight, as well as a sharper drop in the temperature along the blowing axis is predicted after achieving the maximum. But the polymer temperature is still above 90 °C at a take-up distance of 20 cm. At a higher molecular weight of M_w = 250,000 and the same melt extrusion temperature of 190 °C, the filament temperature at the take-up point is lower by about 20 - 30 degrees.

The maximum for the temperature profiles does not appear in the case of the melt extrusion temperature T_0 = 300 °C, equal to the initial temperature of the air jets. The temperature profiles in ***Figure 12*** show a continuous decrease in the polymer temperature along the axis. But the temperature of the polymer still remains above T_m, nearly to the take-up point. Due to the high temperature in the range of effective drawing of the filaments, above or near T_m, no crystallisation along the processing axis is predicted under the conditions discussed, and the filaments are amorphous when they fall onto the take-up plane. The filaments fall onto the take-up plane at zero tensile stress, and thus they should show a rather marginal molecular orientation, if any. The computations indicate that in melt blowing with an initial air jet temperature of 300 °C, crystallisation of the filaments would take place after deposition on the take-up plane, during the cooling of the nonwoven, independently of the melt extrusion temperature.

The axial profiles of the tensile force, tensile stress and rheological pressure provide important and complementary information about the process dynamics. The profiles computed for the molecular weight M_w = 250,000 and melt extrusion temperature T_0 = 300 °C are shown in ***Figures 13 - 15*** for various initial velocities of the air jets. The characteristic feature of the dynamic profiles is the disappearance of the tensile force at the take-up plane. In such a case we should expect a relaxation of the molecular orientation of the filaments falling freely onto the take-up plane, and the fibres in the nonwoven should show rather a marginal molecular orientation. Because the filaments are predicted to be amorphous at the end of the melt blowing axis, crystallisation of the filaments during the cooling of the nonwoven occurs at a marginal molecular orientation, but with possible memory effects of the molecular orientation and thermal history at the crystal nucleation rate [15].

The tensile force profiles in ***Figure 13*** show their maximum at the spinneret, for each of the initial air jet velocities. The maximum occurs as an effect of the accumulation of the air friction forces from the entire filament between the spinneret and the take-up plane. The tensile force profiles and their maxima increase monotonically with an increase in the initial air velocity. The tensile stress profiles (***Figure 14***), contrary to the tensile force profiles, show very low values at the spinneret, and next they increase, approaching the maximum at a distance of about 4 - 6 cm from the spinneret. The tensile stress, after achieving its maximum, decreases to zero at the free end of the filament at the take-up plane. The maximum of the tensile stress increases significantly with an increase in the initial air jet velocity, from about 3 kPa at V_{a0} = 30 m/s through 6 kPa at 50 m/s, 14 kPa at 75 m/s to 1240 kPa at 300 m/s. The maximum tensile stress predicted at a distance away from the spinneret is a consequence of the rapid attenuation of the polymer stream within a narrow range of the processing axis, despite a monotonic decrease in the tensile force from its maximum at the spinneret. The location of the tensile stress maximum corresponds to the maximum of the elongation rate (axial velocity gradient).

Axial profiles of the rheological pressure resulting from the viscoelastic effects in the polymer bulk, computed for different initial velocities of the air jets, are shown ***Figure 15***. The values of the pressure are negative, opposite to the atmospheric pressure, and concentrated within a narrow range of about 1 - 2 cm next to the spinneret. The maximum of the absolute value of the rheological pressure increases with the initial air jet velocity from very low values at lower air jet velocities, i.e. about 0.03 kPa at V_{a0} = 30 m/s, 0.09 kPa at 50 m/s, 0.22 kPa at 70 m/s and 0.46 kPa at 100 m/s, up to 66 kPa at 300 m/s. The position of the maximum shifts from the spinneret by about 2 mm at V_{a0} = 30 m/s to 10 mm at V_{a0} = 300 m/s. The negative rheological pressure acts against the cohesion forces in the polymer bulk within the narrow range near the spinneret.

The computations indicate that with an increase in the initial air jet velocity to high, ultrasonic values, the bending and coiling instability may approach the range of negative rheological pressure and could induce the axial splitting of the filament into nano-filaments, as reported for ultrasonic processing in [16]. Here we are postulating a combined mechanism for splitting the filaments into nanofibers using the rheological pressure as well as the banding and coiling induced in ultrasonic melt blowing.

Conclusions

Computer simulation of the pneumatic melt spinning of isotactic polypropylene on the basis of the mathematical model presented in Part I and II [8, 9] of the publication series leads to the following conclusions concerning the dynamics and mechanism of the process.

1) Two dynamic zones of the air jet-filament interactions are predicted, separated by a critical point of bending and coiling instability at which the air jet and filament axial velocities coincide. Upwards from the critical point, the air-drawing zone of the aligned filaments is predicted to which the air jets coaxially extend the polymer streams, leading to a parallel order of the filaments. Below the point, a bending and coiling zone is predicted where the hampering of the filaments by the air jets occurs due to the excessive axial velocity of the filaments.
2) A different order of the fibres in the nonwoven is expected, depending upon the dynamic zone at which the collector is located, as well as on the velocity of the take-up conveyor. A higher content of structure non-uniformities in the nonwoven should be expected for the case when the take-up is located at the coiling zone, in particular when the filaments are in a liquid state during the coiling on the melt blowing axis. For the collector located in the zone of aligned filaments, the diameter of the fibers in the nonwoven should depend on the take-up distance from the spinneret and should increase with a decrease in the distance. Take-up at distances below the air-drawing zone should not affect the diameter of the fibres, except for a marginal thickening, which is possible as a consequence of strain relaxation or the marginal thinning of some filaments caused by an acceleration in statistical collisions between filaments.
3) The critical point of the bending and coiling instability is affected by the initial velocity of the air jets, the molecular weight of the polymer and the melt extrusion temperature. The coiling zone shifts towards the spinneret with an increasing in the initial air jet velocity, with a higher sensitivity of the critical point to the air velocity in the range of low and intermediate values of the velocity. At very high air jet velocities, approaching the supersonic limit, the bending and coiling instability shifts to very small distances of a few centimeters from the spinneret and approaches the range of negative rheological pressure which acts against the cohesive forces in the polymer bulk. A considerable shift of the instability range to the spinneret is also predicted with a decrease in the melt extrusion viscosity, i.e. with an increasing in the melt extrusion temperature and/or the polymer melt flow rate.
4) The computed axial profiles of the dynamic functions indicate the maximum of the tensile force at the beginning of the processing axis, followed by a monotonic decrease in and disappearance of the force at the take-up plane. Despite the maximum of the tensile force, the tensile stress is marginal at the beginning of the processing axis. Next, it increases due to the rapid attenuation of the polymer stream, approaches the maximum at a distance of about 4 - 6 cm from the spinneret, and reduces to zero at the take-up plane. Axial profiles of the tensile force and tensile stress increase considerably with an increasing in the initial velocity of the air jets. A negative rheological pressure appears in the polymer bulk within a narrow range of about 2 cm adjacent to the spinneret, and a maximum of the absolute value of the pressure is located at a short distance from the spinneret, not exceeding 1 cm.
5) The axial profiles of the filament velocity and diameter indicate that filament formation occurs in the narrow range of 6 - 8 cm next to the spinneret, where the maxima of the elongation rate and tensile stress are predicted. The elongation rate increases, and the diameter of the filament decreases with an increase in the initial air jet velocity, melt extrusion temperature, and the polymer melt flow rate.
6) The axial profiles of the polymer temperature are high and show amorphous filaments at the end of the melt blowing axis in the processing.Locating the collector within the air-drawing zone is recommended to avoid the coiling and interconnection of amorphous filaments on the process axis, leading to non-homogeneities in the nonwoven's structure.
7) In the case of very high initial air jet velocities, approaching the supersonic limit, the air-drawing zone with aligned filaments reduces to a few centimeters, and the take-up of the nonwoven takes place in the bending and coiling zone. To avoid the generation of structure non-homogeneities in the nonwoven, blowing with a much lower initial temperature of the air jets might be recommended. In such a case the air jets could transform the polymer streams to solid filaments by vitrification, or oriented crystallisation, before entering the coiling zone. Also, adjusting the geometry of the die assembly should be necessary to account for the very short zone of aligned filaments.

Acknowledgment

This paper resulted from research supported by Research Grant Nr 3 T08E 08628 from the State Committee for Scientific Research, Poland.

References

1. *Bansal V., Shambaugh R. L.; Ind. Eng. Chem. Res., Vol. 37, 1998, p. 1799.*
2. *Farer R., Batra S. K., Ghosh T. K., Grant E., Seyam A. M.; International Nonwovens J., Spring 2003, p. 36.*
3. *Bresee R. R., Ko W. C.; International Nonwovens J., Summer 2003, p. 21.*
4. *Bresee R. R.; International Nonwovens J., Spring 2004, p. 36.*
5. *Moore E. M., Papavassiliou D. V., Shambaugh R. L.; International Nonwovens J., Fall 2004, p. 43.*
6. *Krutka H. M., Shambaugh R. L., Papavassiliou D. V.; Ind. Eng. Chem. Res., Vol. 42, 2003, p. 5541.*
7. *Chen T., Wang X., Huang X.; Textile Research J., Vol. 74, 2004, p. 1018.*
8. *Zachara A., Lewandowski Z.; Fibres and Textiles in Eastern Europe, Vol. 16 (2008) No. 4(69), p. 17.*
9. *Jarecki L., Ziabicki A.; Fibres and Textiles in Eastern Europe, Vol. 16 (2008) No. 5(70), p. 22.*
10. *Lewandowski Z., Ziabicki A., Jarecki L.; Fibres and Textiles in Eastern Europe, Vol. 15 (2007) No. 5-6 (64-65), p. 77.*
11. *Chen T., Huang X.; Textile Res. J., Vol. 73, 2003, p. 651.*
12. *Chen T., Wang X., Huang X.; Textile Res. J., Vol. 75, 2005, p. 76.*
13. *Press W. H., Flannery B. P., Teukolsky S. A., Vetterling W. T.; „Numerical Recipes", Cambridge Press 1989.*
14. *van Krevelen D. W.; "Properties of Polymers", Third Edition, Elsevier, Amsterdam 2000, p. 676.*
15. *Ziabicki A., Alfonso G. C.; Colloid Polymer Sci., Vol. 272, 1994, p. 1435.*
16. *Gerking L.; Chemical Fibers International, Vol. 52, 2002, p. 424.*

Received 20.02.2008 Reviewed 21.01.2009